

Coated mesh photocatalytic reactor for air treatment applications: comparative study of support materials

**Claudio Passalía, Emanuel Nocetti,
Orlando Alfano & Rodolfo Brandi**

**Environmental Science and Pollution
Research**


ISSN 0944-1344

Environ Sci Pollut Res
DOI 10.1007/s11356-016-7057-7



Your article is protected by copyright and all rights are held exclusively by Springer-Verlag Berlin Heidelberg. This e-offprint is for personal use only and shall not be self-archived in electronic repositories. If you wish to self-archive your article, please use the accepted manuscript version for posting on your own website. You may further deposit the accepted manuscript version in any repository, provided it is only made publicly available 12 months after official publication or later and provided acknowledgement is given to the original source of publication and a link is inserted to the published article on Springer's website. The link must be accompanied by the following text: "The final publication is available at link.springer.com".

Coated mesh photocatalytic reactor for air treatment applications: comparative study of support materials

Claudio Passalía^{1,2} · Emanuel Nocetti¹ · Orlando Alfano^{1,3} · Rodolfo Brandi^{1,3} Received: 29 February 2016 / Accepted: 7 June 2016
© Springer-Verlag Berlin Heidelberg 2016

Abstract An experimental comparative study of different meshes as support materials for photocatalytic applications in gas phase is presented. The photocatalytic oxidation of dichloromethane in air was addressed employing different coated meshes in a laboratory-scale, continuous reactor. Two fiberglass meshes and a stainless steel mesh were studied regarding the catalyst load, adherence, and catalytic activity. Titanium dioxide photocatalyst was immobilized on the meshes by dip-coating cycles. Results indicate the feasibility of the dichloromethane elimination in the three cases. When the number of coating cycles was doubled, the achieved conversion levels were increased twofold for stainless steel and threefold for the fiberglass meshes. One of the fiberglass meshes (FG2) showed the highest reactivity per mass of catalyst and per catalytic surface area.

Keywords Indoor pollution · Heterogeneous photocatalysis · Dichloromethane · Mesh reactor · Efficiency

Introduction

Indoor air pollution is a major issue nowadays. People spend most of their time in confined places and are exposed to a wide

Responsible editor: Suresh Pillai

✉ Rodolfo Brandi
rbrandi@santafe-conicet.gov.ar

¹ Facultad de Ingeniería y Ciencias Hídricas, Universidad Nacional del Litoral (FICH-UNL), Ciudad Universitaria, 3000 Santa Fe, Argentina

² Consejo Nacional de Investigaciones Científicas y Técnicas (CONICET), Buenos Aires, Argentina

³ Instituto de Desarrollo Tecnológico para la Industria Química, INTEC (CONICET-UNL), Güemes, 3450 Santa Fe, Argentina

variety of chemical compounds (Jones 1999). Among them, volatile organic compounds (VOCs) represent a major source of indoor contamination. In recent years, there has been a particular interest on the halogenated family of VOCs which may be released by a number of household and office materials (Kowalska et al. 2015). VOCs, in general, and chlorinated ones in particular, are responsible for a number of chronic health effects when they are present in confined environments.

In order to reduce the exposure levels to VOCs, the advanced oxidation technologies of proven efficiency in air treatment could be used. In particular, photocatalytic wall reactors have been successfully applied in the control of air pollutants (Boonen and Beeldens 2014). Some works, however, showed that halogenated aliphatic hydrocarbons present the lowest photocatalytic conversion efficiencies when compared to other VOC types (Hodgson et al. 2007).

Dichloromethane (CH_2Cl_2), also known as methylene chloride, is a chlorinated aliphatic hydrocarbon compound. This organic compound is one of the most typical indoor air pollutants; it is usually found in concentrations several times larger than outdoors (Nero 1988). Dichloromethane (DCM) can be found either in domestic or industrial environments because it is used in the production of many products (such as paint stripper, pharmaceuticals, and as a solvent) and in consumer products like hair-spray aerosols, household cleaning products, room deodorants, etc. The diverse nature of its application implies that dichloromethane can be released to the environment to a large extent.

Although dichloromethane has a moderate toxicity level, it can produce adverse health effects to humans. The principal route of human exposure to this compound is inhalation of ambient air (USEPA 2000). Chronic inhalation exposure to dichloromethane can produce headaches, dizziness, nausea, and memory loss. Furthermore, dichloromethane is classified as a potential carcinogenic to humans. The permitted exposure level in workplaces was established at 25 ppm.

Along with other chlorinated methanes, dichloromethane was used as a target pollutant in the investigation of heterogeneous photocatalysis. A number of published works dealt with the determination of a reaction pathway. Abu Bakar et al. (2010) studied doped and pure TiO_2 catalysts for the elimination of dichloromethane and similar chlorinated hydrocarbons; they found a degradation level for dichloromethane in between those of chloroform and carbon tetrachloride. Yu et al. (2012) studied the photodegradation of dichloromethane in different reaction media and detected small quantities of organic intermediates; based on their experimental findings, they proposed a probable degradation pathway. The identification and quantification of significant quantities of intermediates was also performed by Borisch et al. (2004). In their work, high initial concentrations of dichloromethane in a batch system were used to report the presence of carbon monoxide, chloroform, and formyl chloride, among other intermediates.

Among the possible photocatalytic wall reactor configurations, the photocatalytic mesh reactors have a special feature: they provide a media that absorbs the radiation that initiates the degradation reaction while allowing a certain fraction of the radiation flux to pass through the mesh. This transmitted radiation fraction can be further intercepted by another contiguous mesh and be used for the superficial reaction. In addition, the photocatalytic mesh reactor provides a good contact area between the air and catalyst with a minimum pressure drop. Because of these advantages, there have been some recent focuses on the coated mesh photocatalytic gas phase reactor. Taranto et al. (2009) compared honeycomb monolith and mesh reactors regarding pollutant degradation and pressure drop; Chang et al. (2010) studied a coated stainless steel sieve for elimination of acetone; Ochiai et al. (2011) addressed a modified titanium mesh filter for odour control in batch and continuous mode. The radiative interchange modelling and experimental validation of a multiple mesh photocatalytic reactor for air remediation has been previously addressed (Esterkin et al. 2005).

The selection of the support material for such a mesh reactor is crucial, given that the optical properties (transmittance and absorbance), the superficial catalyst load, the coating adherence and the mechanical and chemical stability of the catalytic mesh have a direct effect on the photocatalytic reactor performance.

Our research is currently centered on the selection of mesh materials for reaching an efficient dichloromethane removal from air. The aim of this work is to evaluate and compare the performance of different substrate materials for a coated mesh photocatalytic reactor, using titanium dioxide (TiO_2) as photocatalyst and near UV lamps for the elimination of dichloromethane.

Materials and methods

Support materials

Three low-cost materials were chosen for the immobilization of the catalyst (Fig. 1): two fiberglass meshes and a stainless steel mesh. Besides their composition materials, the meshes differ in their wire diameter and opening sizes; main characteristics of the meshes are presented in Table 1. The variable open area fraction (OAF) on the last column of Table 1, is the ratio of open area to total mesh area at a normal angle of incidence to the plane of the material.

All three materials were chosen for their market availability. Rectangular samples of each mesh were used for the determination of catalyst loading, optical properties, and photocatalytic activity tests. Before the catalyst immobilization each piece was cleaned with distilled water, rinsed and dried; in addition, they were cleaned with acetone and dried in stove at 40 °C. A further treatment was needed for one of the commercially available meshes, FG1, which is coated with PVC; this plastic was eliminated thermally by exposing the mesh during a 6-h period in a muffle; the temperature rate of the first hour was 3.5 °C/min, followed by a 1 °C/min ramp for 5 further hours. The final temperature was 600 °C.

Catalyst immobilization

The catalyst was immobilized onto the meshes by a series of dip-coating cycles. A suspension of 50 g/L of pure titanium dioxide was prepared with distilled water. Aeroxide P25 (from Evonik, Germany) was employed without further treatment. This commercial catalyst is composed mainly of crystalline TiO_2 with an anatase/rutile ratio of 5.5, and around a 10.0 wt% amorphous phase (Ohtani et al. 2010; Tobaldi et al. 2014). Prior to each coating cycle, the suspension was kept for 1 h in a magnetic stirrer to homogenize the catalyst concentration.

Each mesh was immersed in a vessel containing the suspension which was recirculated and mixed by means of a peristaltic pump. After 1 min, the vessel was evacuated at a controlled velocity of 10 cm/min. Once extracted, the mesh

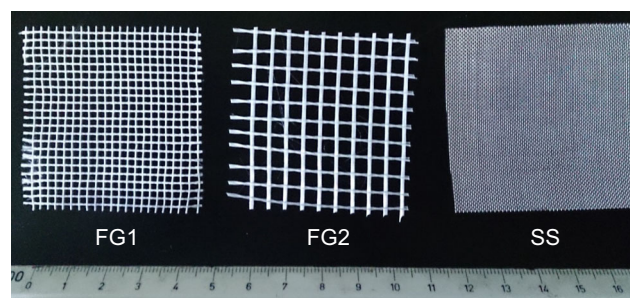


Fig. 1 Photograph of the tested meshes. FG1 and FG2 are fiberglass meshes; SS is the stainless steel mesh. The length scale is in cm

Table 1 Mesh properties

Material	Mesh size ^a	Weight (g/m ²)	OAF
FG1	10	114.4	0.60
FG2	5	102.7	0.67
SS	25	876.2	0.45

OAF open area fraction

^a US Standard size

was let to dry and then put in the stove at 80 °C for 1 h. In the case of the stainless steel mesh, an additional 5-h calcination period at 300 °C followed the drying process. The coating procedure was repeated a number of times to increase the amount of fixed catalyst.

Reactor

The reactor itself is made in acrylic and holds inside the coated mesh. In order to avoid mass transfer limitations to the catalyst surface, the reactor thickness is only 6 mm and the mesh is located at the midpoint between windows. The near UV radiation sources are two sets of actinic lamps (Sylvania F15W T12) which provide a uniform flux over the reactor windows. The reactor dimensions and operating conditions are summarized in Table 2.

Dichloromethane source and analytical determination

Pure dichloromethane gas was delivered by a custom-made pressurized gas cylinder. Firstly, a gas tube is evacuated by means of a vacuum pump. In the second place, an aliquot of the pure liquid dichloromethane (Sintorgan, reagent grade) is introduced into the tube aided with a syringe and by opening the tube's valve for a few seconds. Finally, the tube is connected to an air compressor and then filled with air up to a pressure of 120 psi.

Table 2 Reactor dimensions and operating conditions

Reactor dimensions		
Thickness (T)	0.6	cm
Length (L)	10	cm
Width (W)	15	cm
Mesh total area	150	cm ²
Operating conditions		
Relative humidity	5 ± 1	%
Temperature	22 ± 2	°C
Inlet DCM concentration	65.6 ± 2.4	ppmv
Feed flow rate	1	L min ⁻¹
Maximum radiation level	28	W m ⁻²
Radiation wavelengths range	300–400	nm

Concentrations of dichloromethane at the inlet and outlet of the reactor are determined from gas-tight syringe extracted samples by gas chromatography. The gas chromatograph (HP 5890) was operated in splitless mode using nitrogen as a carrier; the injector temperature was set at 170 °C, the detector at 250 °C and the oven at constant 40 °C. In a previous step, a calibration curve of dichloromethane response in GC-FID was made applying a static headspace method (Kolb and Ettre 1997).

Reactor operation

The reaction system layout is presented in Fig. 2. The reactor operates in continuous mode, in one pass with no recycle. The pneumatic circulation is provided by a compressor; the air stream is passed through a filtration system composed by two granular bed columns of activated carbon and silica gel. The desired dichloromethane concentration at the reactor inlet is obtained by adequate regulation of mass flow controllers. A continuous air stream feeds the reactor with a known concentration of dichloromethane and relative humidity. Inside the reactor, a manifold system was placed to obtain a uniform flow over the reactive mesh.

An experimental run is performed as follows: before the mesh is irradiated, the air containing the pollutant is circulated in the reactor until the inlet and outlet concentration reach a constant value. Once a steady-state condition is obtained, the irradiation period is started; the outlet concentration is measured over time and the conversion is calculated when no significant change is observed.

The absolute irradiance level at the reactor windows was determined with a portable spectrophotometer (Ocean Optics USB2000+UV-VIS-ES). The optical properties of the meshes, total reflectance, and transmittances were determined in a laboratory spectrophotometer with integrating sphere (Optronic OL50).

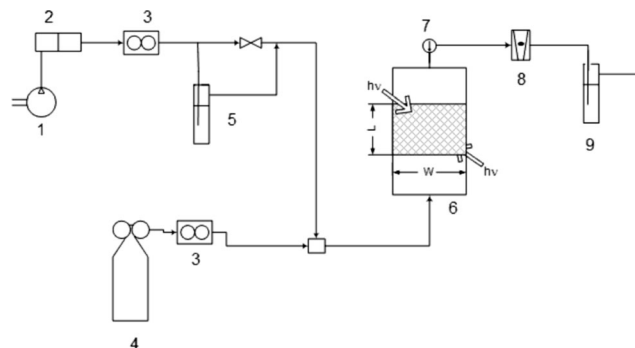


Fig. 2 Experimental reaction setup: 1, air compressor; 2, air filter with activated carbon and silica gel; 3, mass flow controller; 4, cylinder with DCM in air mixture; 5, humidifier; 6, photo-reactor; 7, sample port; 8, variable area flowmeter; 9, wet scrubber

Results and discussion

Coating morphology

A microscopic inspection of the coatings over the different substrates was performed. Samples of the coated meshes were examined under a scanning electron microscope (SEM; Jeol JSM-35C); the selected images are shown in Fig. 3.

From the microscopic images of the meshes with four coating cycles, it can be seen that in each case the coating coverage over the substrate is high. In addition, as can be seen in the case of the stainless steel (SS b) mesh, the thickness of the catalyst layer is in the order of 10 μm .

Catalyst load

One of the first parameters evaluated was the catalyst load on the different meshes. This was achieved by registration of mesh samples weight after each immobilization cycle, i.e., dip-coating, drying (and calcination for the stainless steel mesh). As can be seen in Fig. 4, the amount of catalyst fixed

is proportional to the number of cycles, but the differential mass added becomes lower as the number of cycles increases for some materials. After four depositions, the sample meshes were observed to have a proper spatial uniformity in sight and no observable uncoated spots. The reported catalyst loads in Fig. 4 are computed considering the total geometric area of the samples, all of which are square pieces of 5 cm in side.

As can be seen in Fig. 4, there is a complete different behavior of the substrates and the final load achieved for the FG1 is the largest, while for FG2 is lowest. An intermediate behavior is observed with the mesh of stainless steel. Meshes with two and four coating cycles were used in the activity and adherence tests.

Catalyst adherence test

In order to provide an additional parameter for the substrate comparison, a test for catalyst adherence was performed. Even though the coated materials are to be used with gaseous streams, the adherence of the catalytic layers to the substrate was evaluated in aqueous medium using the ultrasonic

Fig. 3 SEM images of the meshes after four coating cycles

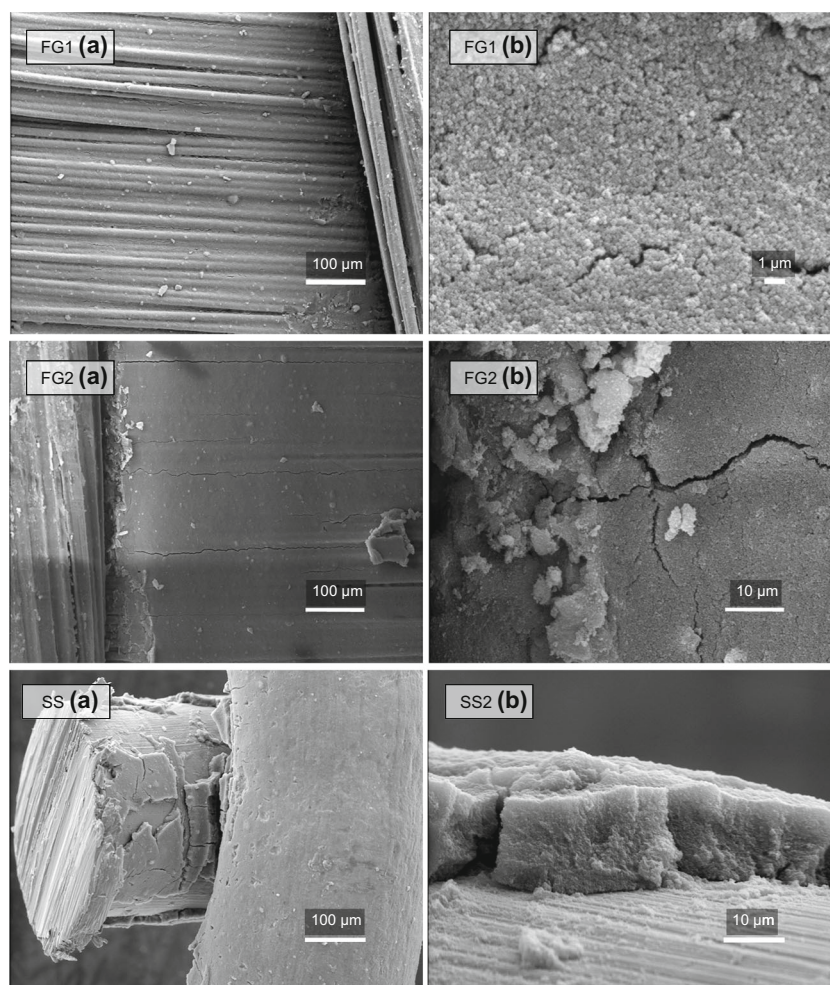
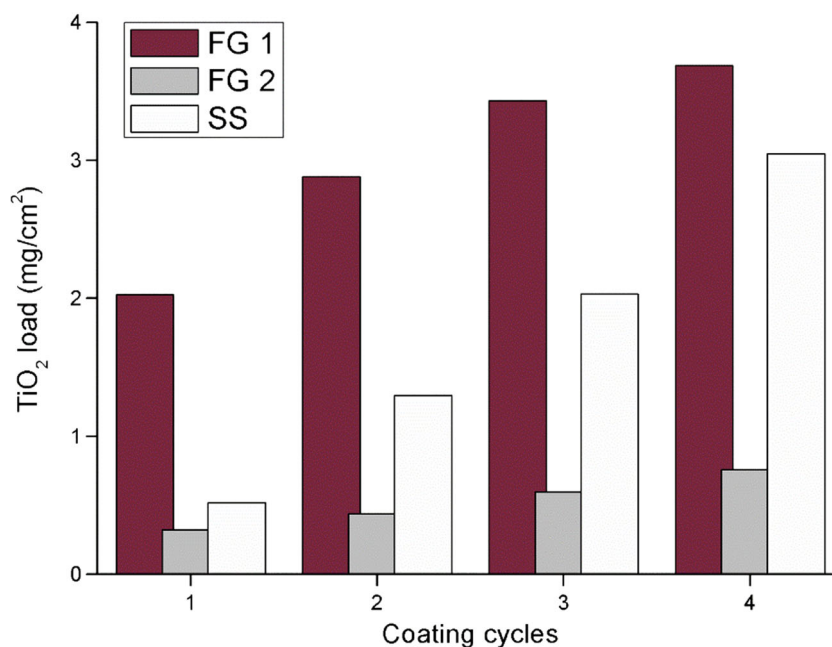


Fig. 4 Catalyst load after each coating cycle

method, as described in the literature (Martínez et al., 2009). It consists in the measurement of the weight loss caused by the exposition of the sample to ultrasound. The coated meshes immersed in distilled water were submitted to an ultrasonic treatment in a Neyo Ultrasonik 300 for 30 min at room temperature and maximum power. After that, the samples were dried in a stove at 80 °C for 2 h. The weight loss was determined by the difference in the mass of the samples before and after the ultrasonic test, and adherence results are presented in Table 3 in terms of the remaining TiO₂ mass percentage.

As can be seen in Table 3, there is an appreciable catalyst loss after 30 min of sonication, being FG1 the material with least adherence. Nevertheless, it is worth mentioning that this testing method exerts a higher stress to the materials than in the desired gas-phase operation; in fact, no catalyst detachment was observed during the photocatalytic activity tests.

Optical properties

The total spectral reflectance and transmittance of the uncoated support materials and the coated meshes were measured in

Table 3 Adherence of catalyst

Sample	# of cycles	TiO ₂ load (mg/cm ²)	Adherence (%)
FG1	2	2.88	53.8
	4	3.68	43.1
FG2	2	0.44	61.5
	4	0.76	68.8
SS	2	1.29	63.2
	4	3.05	62.9

the wavelength range of emission power of the lamps, i.e., 300–400 nm. See for instance Fig. 5a, where the optical properties for FG1 are depicted. The reflectance of the coated meshes is lower than the reflectance of the uncoated substrate for wavelengths below 390 nm approximately, as a result of the well-known limit for TiO₂ absorbance. In addition, the transmittance of the sample has a smooth wavelength dependence and, as can be noted, the spectral value gets slightly lowered for increasing catalyst load. The optical responses of the two fiberglass meshes are similar; on the other hand, the transmittance of the stainless steel mesh has a stronger dependence with the catalyst loading. This behavior may be explained by the low value of the OAF which, in turn, gets lower when the mesh is coated with the titanium dioxide.

Photocatalytic activity tests

Regarding specifically the degradation of dichloromethane in the reaction device, a series of blank tests were performed. In the first place, an analytical screening of the air supplied by the purification system presented no peaks in the chromatogram, indicating the absence of unwanted substances. Secondly, a blank test for photolysis was performed by circulating the dichloromethane mixture in the reactor with uncoated mesh inside (without catalyst) and irradiated with the maximum power. Finally, an additional test was done using the TiO₂-coated mesh inside the reactor but no radiation source. None of these tests presented a significant difference between the inlet and outlet concentrations of dichloromethane, indicating the absence of photolysis and adsorption phenomena under steady-state operation.

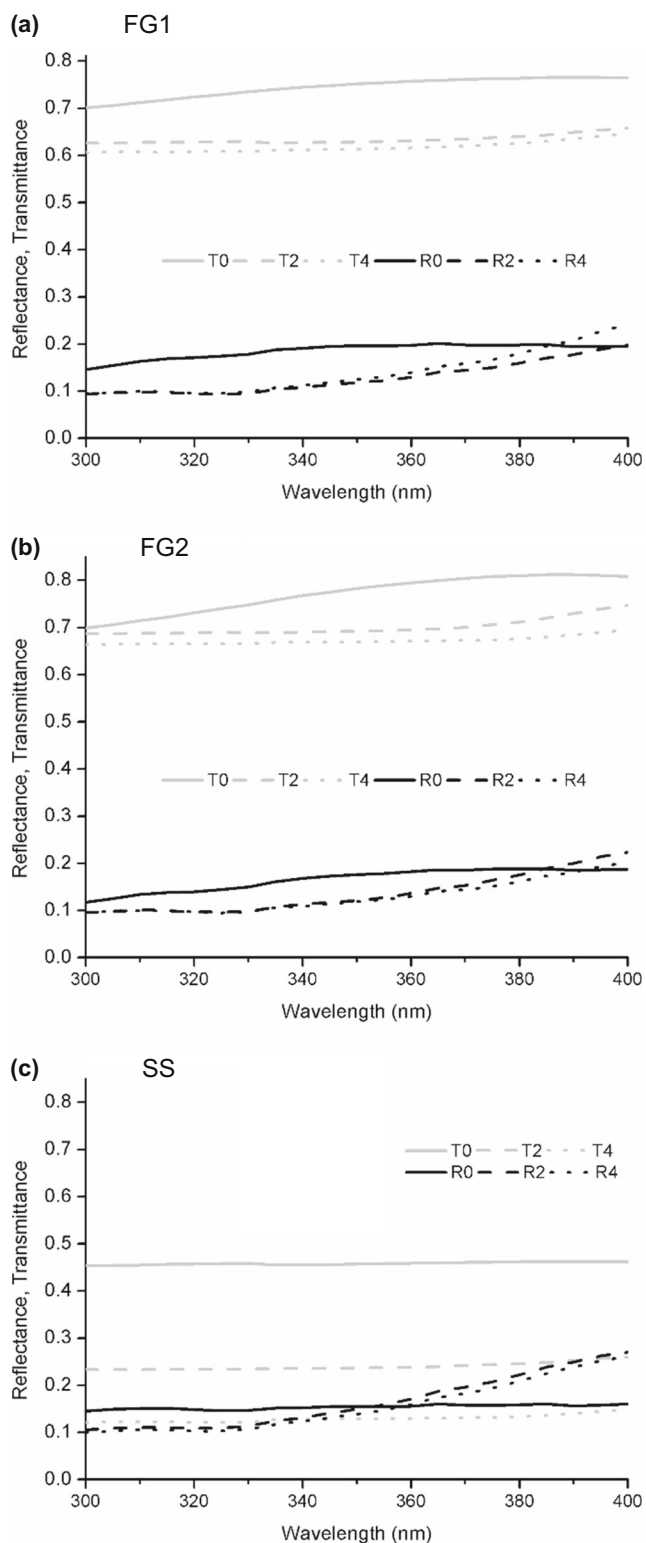


Fig. 5 Optical properties of coated and uncoated meshes. Key: T = transmittance; R = reflectance; 0, uncoated material; 2, mesh with two coating cycles; 4, mesh with four coating cycles

A set of experimental runs were conducted by variation of the substrate material and the catalyst coating cycles. In order to make the results comparable, all operating variables were

kept constant: inlet dichloromethane concentration, total flow rate, radiation flux, and relative humidity. Also, the different samples had identical dimensions. The details for each of the values of operating conditions are summarized in Table 2.

Even though we were only interested in the degradation of dichloromethane, it is worth noting that the only identified compound at the reactor outlet, other than dichloromethane, was chloroform. The identification was performed by comparing the retention times in the chromatograms of samples taken at the reactor outlet with the ones of headspace samples injections of pure chloroform. To give an idea of the amount of products at the reactor outlet, the area counts for chloroform were at least three orders of magnitude lower than those of dichloromethane. The presence of chloroform as a reaction intermediate is consistent with the proposed kinetic pathway of Borisch and coworkers (Borisch et al. 2004).

In order to obtain an activity test free of external mass transfer limitations, the experiments were carried out under operating conditions that satisfied the criterion that relates at the steady state the observed reaction rate and the mass transfer of dichloromethane in air (Passalía et al. 2010):

$$\frac{\langle r_{DCM} \rangle_{obs}}{k_m C_{in}} \leq 0.1 \quad (1)$$

where k_m is a mass transfer coefficient. The observed removal rate ($\text{mol cm}^{-2} \text{s}^{-1}$) was computed as

$$\langle r_{DCM} \rangle_{obs} = \frac{Q(C_{in} - C_{out})}{A_{cat}} \quad (2)$$

where Q is the volumetric air flow rate ($\text{cm}^3 \text{s}^{-1}$), C_{in} and C_{out} are the inlet and outlet dichloromethane concentrations, respectively (mol cm^{-3}), and A_{cat} is the catalytic area (cm^2). The mass transfer coefficient (cm s^{-1}) was estimated through the experimental correlation of Uberoi and Pereira (1996) for monolith reactors:

$$k_m = 2.696 \frac{D_{ab}}{d} \left(1 + 0.139 Sc Re \frac{d}{L} \right)^{0.81} \quad (3)$$

where Sc and Re are the Schmidt and Reynolds numbers, respectively, D_{ab} is the binary diffusivity of dichloromethane in air, and d is the characteristic length of the system. For the studied operating conditions and reactor dimensions, the value of k_m obtained was $0.85 \text{ (cm s}^{-1}\text{)}$; with this value, the criterion is fully satisfied, being always below $0.02 < 0.1$.

In Fig. 6, a typical experimental result for the stainless steel mesh is shown. Samples are taken for determination of the inlet and outlet concentrations until their difference seems to be stable. Although low conversion levels were generally found under the adopted operating conditions, the results are consistent with the reactor scale and the low catalytic area available. Recall also that the residence time is only 5.4 s.

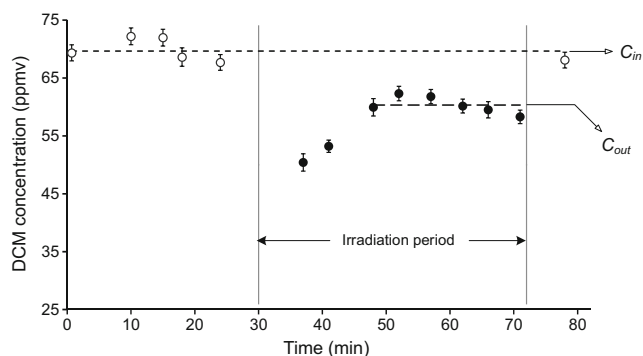


Fig. 6 Photocatalytic test for SS mesh with two coating cycles

It is noticeable from Fig. 6 that, in the first moments of the irradiated period, the outlet dichloromethane concentration is the lowest and then it stabilizes in a larger value. This variation of the observed removal rate may be due to a dynamic adsorption phenomenon over the catalyst surface and is consistent with previous findings in the literature (Lewandowski and Ollis 2003).

The steady-state outlet concentrations are used for computing dichloromethane conversions for each sample. Table 4 summarizes the set of experimental runs for the six mesh samples. As can be observed, a certain dichloromethane reduction level could be achieved in all cases.

When comparing global conversion levels (third column), the FG1 sample with four coating cycles shows the best performance. In every case, the conversion for the samples with four coating cycles is larger than for samples with two cycles; this effect goes along with the increase in TiO_2 load. For the case of dichloromethane reduction per catalyst mass (sixth column), FG2 showed the largest output, being the highest value 135 ppb/mg. In addition, the concentration reduction per catalytic surface area is presented and high conversion levels are also obtained for FG2. Note that the catalytic area is computed as twice the normal solid to total area, $A_{\text{cat}} = 2A_n(1 - OAF)$.

According to the obtained results, although the FG2 mesh has the lowest catalyst load and active area, it shows the best dichloromethane reduction per TiO_2 mass and also a high dichloromethane reduction per catalytic area. This is a significant finding given that FG2 is also the lightest support material and the one with largest open area fraction.

Qualitative analysis

Stainless steel mesh is an appropriate material for the immobilization of TiO_2 , particularly for having the structural capacity of maintaining a certain form and aiming for a larger scale, multiple-mesh reactor configuration. Nevertheless, one drawback of this material is the appearance of corrosion points that were observed after prolonged reaction tests. This phenomenon can be explained in view of the chemical nature of this chlorinated compound, but most likely for the production of HCl in the surface. Hydrogen chloride is the end-product of the mineralized dichloromethane molecule.

Of the two fiberglass meshes, FG1 has the problem of loose and labile structure, which makes it difficult to keep the desired form within the reactor. This problem may become even worse when dealing with larger pieces of mesh for a reactor of bigger dimensions.

From this experimental comparative study of the different meshes assessed, it can be concluded that FG2 is the most appropriate mesh for the scaling up to a larger reactor for photocatalytic air purification.

Conclusions

Three meshes of different materials were tested as substrates for immobilization of photocatalyst and their application for gas-phase pollution control. All three samples (two fiberglass and one stainless steel meshes) were coated with titanium dioxide and were able to reduce dichloromethane concentration in one pass. Adequate conversion levels were obtained in our laboratory-scale continuous reactor. Chloroform was the only reaction intermediate identified, but in concentration orders of magnitude lower than those of dichloromethane.

Because of its poor catalyst adherence capability and labile structure, FG1 can be disregarded for further applications at a larger scale. On the other hand, FG2 shows a much better efficiency and can hold its shape better than FG1. Stainless steel performs well regarding photocatalytic reactivity and has the best mechanical strength; this coated metal mesh has the lowest transmittance, which may be a drawback for a multiple mesh configuration. In addition, stainless steel is the most

Table 4 Photocatalytic activity tests and efficiencies

Material	# of coating cycles	DCM conversion (%)	TiO_2 load, m_{cat} (mg)	Catalytic area, A_{cat} (cm^2)	$\Delta C/m_{\text{cat}}$ (ppb/mg)	$\Delta C/A_{\text{cat}}$ (ppb/ cm^2)
FG1	2	10.0 ± 4.1	432.0	120	15.0	54.2
	4	37.2 ± 4.2	552.6	132	45.4	190.2
FG2	2	7.1 ± 2.9	65.4	102	68.8	44.1
	4	23.6 ± 2.7	113.4	105	134.9	145.7
SS	2	15.1 ± 3.0	193.8	174	54.2	60.3
	4	32.7 ± 2.5	457.2	180	45.9	116.7

expensive of the three materials tested and presents corrosion points after prolonged reaction tests.

This study is intended to be a starting point toward the intrinsic kinetic of dichloromethane destruction from a kinetic pathway and, ultimately, to a scaling up of the photocatalytic reactor for the treatment of larger air volumes.

Acknowledgments The authors are grateful to the Universidad Nacional del Litoral (UNL), Consejo Nacional de Investigaciones Científicas y Técnicas (CONICET), and Agencia Nacional de Promoción Científica y Tecnológica (ANPCyT) of Argentina for the financial support. The technical assistance of Antonio C. Negro is also acknowledged.

References

- Abu Bakar W, Ali R, Othman M (2010) Photocatalytic degradation and reaction pathway studies of chlorinated hydrocarbons in gaseous phase. *Trans C Chem Chem Eng* 17(1):1–14
- Boonen E, Beeldens A (2014) Recent photocatalytic applications for air purification in Belgium. *Coatings* 4:553–573
- Borisch J, Pilkenton S, Miller M, Raftery D, Francisco J (2004) TiO₂ photocatalytic degradation of dichloromethane: an FTIR and solid-state NMR study. *J Phys Chem B* 108:5640–5646
- Chang C, Lee Y, Lin C, Lee J, Chang Y, Chen J (2010) Degradation of volatile acetone by a photocatalytic reactor with TiO₂ coated sieve. *Adv. Mater Res* 123-125:919–922
- Esterkin CR, Negro A, Alfano O, Cassano A (2005) Air pollution remediation in a fixed bed photocatalytic reactor coated with TiO₂. *AICHE J* 51(8):2298–2310. doi:10.1002/aic.10472
- Hodgson AT, Destailhats H, Sullivan DP, Fisk WJ (2007) Performance of ultraviolet photocatalytic oxidation for indoor air cleaning applications. *Indoor Air* 17:305–316
- Jones A (1999) Indoor air quality and health. *Atmos Environ* 33:4535–4564
- Kolb B, Ettore L (1997) Static headspace-gas chromatography. Theory and practice. Wiley-VCH, New York
- Kowalska J, Szczyńska M, Pośniak M (2015) Measurements of chlorinated volatile organic compounds emitted from office printers and photocopiers. *Environ Sci Pollut Res* 22:5241–5252
- Lewandowski M, Ollis D (2003) A two-site kinetic model simulating apparent deactivation during photocatalytic oxidation of aromatics on titanium dioxide (TiO₂). *Appl Catal B* 43:309–327
- Martínez LM, Sanz O, Domínguez MI, Centeno MA, Odriozola JA (2009) AISI 304 Austenitic stainless steels monoliths for catalytic applications. *Chem Eng J* 148(1):191–200
- Nero AV Jr (1988) Controlling indoor air pollution. *Sci Am* 258(5):42–48
- Ochiai T, Niitsu Y, Kobayashi G, Kurano M, Serizawa I, Horio K, Nakata K, Murakami T, Morito Y, Fujishima A (2011) Compact and effective photocatalytic air-purification unit by using of mercury-free excimer lamps with TiO₂ coated titanium mesh filter. *Catal Sci Technol* 1:1328–1330
- Ohtani B, Prieto-Mahaney O, Li D, Abe R (2010) What is Degussa (Evonik) P25? Crystalline composition analysis, reconstruction from isolated pure particles and photocatalytic activity test. *J Photochem Photobiol A* 216(2–3):179–182
- Passalía C, Martínez Retamar E, Alfano O, Brandi R (2010) Photocatalytic degradation of formaldehyde in gas phase on TiO₂ films: a kinetic study. *Int J Chem React Eng* 8(A161). doi:10.2202/1542-6580.2494
- Taranto J, Frochot D, Pichat P (2009) Photocatalytic air purification: comparative efficacy and pressure drop of a TiO₂-coated thin mesh and a honeycomb monolith at high air velocities using a 0.4 m³ close-loop reactor. *Sep Purif Technol* 67:187–193
- Tobaldi DM, Pullar R, Seabra M, Labrincha J (2014) Fully quantitative X-ray characterisation of Evonik Aeroxide TiO₂ P25®. *Mater Lett* 122:345–347
- Uberoi M, Pereira C (1996) External mass transfer coefficients for monolith catalysts. *Ind Eng Chem Res* 35:113–116
- US EPA (2000) Hazard summary for methylene chloride. <http://www.epa.gov/airtoxics/hlthef/methylen.html>. Accessed 30 May 2016
- Yu J, Chen J, Feng L, Jiang Y, Cheng Z (2012) Conversion characteristics and mechanism analysis of gaseous dichloromethane degraded by a VUV light in different reaction media. *J Environ Sci* 24(10):1777–1784